International Medicine
www.theinternationalmedicine.org

Research Article

Section: Radiodiagnosis

Role of MRI in Differentiating Benign and Malignant Ovarian Tumors

Dr. Kabil Kumar[*1]

[1] M.B.B.S., DNB, Department of Radiodiagnosis, Pushpagiri Institute of Medical Sciences

ARTICLE INFO

Article History:

Received: 28-12-2024

Accepted: 01-02-2025

Keywords:

Magnetic resonance imaging (MRI)

Ovarian tumors

Benign lesions

Malignant lesions

Contrast-enhanced MRI

Adnexal masses

***Corresponding author:**
Dr. Kabil Kumar
M.B.B.S., DNB, Department of Radiodiagnosis, Pushpagiri Institute of Medical Sciences

ABSTRACT

Introduction: Ovarian cancer is a major health challenge globally and ranks as the third most common cancer among women in India. Despite advancements in diagnostics, its poor prognosis persists due to late-stage diagnosis. Early and accurate differentiation between benign and malignant ovarian tumors is essential for improving management and outcomes. Magnetic resonance imaging (MRI) has emerged as a superior modality for characterizing ovarian tumors, offering high sensitivity and specificity compared to ultrasound and computed tomography. **Aim:** This study aimed to determine the sensitivity and specificity of contrast-enhanced MRI in differentiating benign and malignant ovarian tumors, using histopathology as the gold standard. Additionally, the study evaluated MRI imaging characteristics of individual ovarian neoplasm types confirmed by histopathology. **Methods:** This prospective study was conducted over 18 months at Pushpagiri Medical College, including 74 patients with suspected ovarian neoplasms. MRI was performed using a 1.5 Tesla scanner with T1W, T2W, T2 FS, and post-contrast T1 FS sequences. Lesions were classified as benign or malignant based on size, cystic or solid, wall and septal thickness, internal contents and enhancement patterns, with histopathology serving as the reference standard. **Results:** Of the 74 cases, 62 were benign and 12 were malignant. Benign lesions exhibited thin walls, unilocular or multiloculated morphology, and peripheral enhancement. Malignant lesions demonstrated irregular thick walls, thick septae, solid components, and ancillary features like ascites, lymphadenopathy, peritoneal or omental deposits. MRI achieved a sensitivity of 100 % and specificity of 97 % in differentiating these lesions. **Conclusion:** MRI is a useful preoperative test for predicting the diagnosis of ovarian masses. The differentiation of benign from malignant ovarian tumours is of great value because the therapeutic approach is different for each entity. Benign ovarian masses can be managed with more conservative approaches, either with close observation or with laparoscopic surgery. On the contrary, when a tumor is malignant, there is a need for urgent laparotomy.

INTRODUCTION

Ovarian cancer is a significant health concern globally and is particularly alarming in India, where it ranks as the third most common cancer among women after cervical and breast cancer [1]. The age-adjusted incidence rates of ovarian cancer in India vary between 5.4 and 8.0 per 100,000 population, highlighting the geographic and demographic variability of its occurrence [2]. Despite advances in diagnostic and therapeutic modalities, ovarian cancer continues to have the poorest prognosis among gynecological malignancies, with an overall 5-year survival rate of approximately 50% [3]. This dismal statistic is largely attributed tothe advanced stage of disease at diagnosis, inadequate management strategies, and poor compliance with therapeutic protocols.

Given that most patients present with distant or widespread disease at the time of diagnosis, early detection and precise characterization of ovarian masses are critical to improving outcomes. Imaging plays a pivotal role in the evaluation of adnexal masses, with the primary aim of detecting malignancy. Ultrasound (US) is widely regarded as the first-line imaging modality for assessing and

characterizing adnexal lesions [4]. However, its specificity in diagnosing benign ovarian lesions has been reported to be variable, ranging from 60% to 98%. Moreover, as many as 20% of adnexal lesions in premenopausal women remain indeterminate even when ultrasound findings are interpreted alongside clinical parameters and CA-125 levels [5].

Magnetic Resonance Imaging (MRI) has emerged as a superior modality for characterizing ovarian tumors, demonstrating high potential in differentiating between benign and malignant lesions [6]. Contrast-enhanced MRI, in particular, has been shown to achieve an accuracy of 93% in detecting benign lesions and 95% for malignant lesions. Comparative studies have established that MRI outperforms both ultrasound and computed tomography (CT) in preoperative characterization of adnexal masses. For instance, while ultrasound achieves a sensitivity of 53%-88% and CT reaches 66%-94%, MRI demonstrates a higher sensitivity (91%-100%) and specificity (91%-92%) for detecting malignancy.

The role of MRI is not limited to differentiation between benign and malignant tumors but extends to the characterization of specific ovarian pathologies. Serous ovarian cystadenomas are unilocular and frequently bilateral, occurring in 12%-23% of cases, and often exhibit solid characteristics like papillary projections, whereas mucinous cystadenomas are mupltilocualr with differential signal intensity of the cystic components, Endometriotic cysts can be reliably identified on MRI with a sensitivity of 82%-90% and a specificity of 91%-98%[7], based on their signal characteristics, shade sign, multiplicity, and fibrous adhesions [8]. MRI also provides valuable insights into the malignant transformation of ovarian teratomas, with findings such as fat-containing tumors and solid components extending transmurally and invading adjacent pelvic structures [9].

Intravenous gadolinium contrast is particularly useful in assessing malignant components of ovarian tumors, although it is not essential for characterizing fibromas or Brenner tumors when typical signal intensities are present [10]. However, contrast-enhanced studies may be indispensable for determining the extrauterine origin of a solid mass. For endometriosis-associated ovarian cancers, MRI findings such as multilocularity, mural nodules, or foci in chocolate cysts warrant consideration for neoplastic transformation.

Numerous studies have underscored the reliability of MRI in preoperative evaluation of ovarian masses. For instance, Stevens et al. demonstrated that MRI achieved a 95% detection rate of surgically proven adnexal lesions, comparable to CT (96%) and ultrasound (91%) [11]. Similarly, reported high sensitivity and specificity for MRI in differentiating endometriotic cysts from hemorrhagic adnexal lesions. Such evidence reinforces the growing consensus that MRI is a robust imaging tool for evaluating ovarian masses [12].

MRI provides unparalleled accuracy in differentiating benign from malignant ovarian tumors, offering critical info-rmation that aids in preoperative planning and management. Its ability to provide detailed tissue characterization, high sensitivity, and specificity makes it an indispensable modality in the diagnostic armamentarium for ovarian tumors. This study explores the pivotal role of MRI in the characterization of ovarian masses, with a focus on its efficacy in distinguishing benign from malignant lesions.

MATERIALS AND METHODS

This prospective 18-month study, conducted at Pushpagiri Medical College, evaluated patients with suspected ovarian neoplasms using MRI, surgery, and histopathology. Exclusion criteria included refusal to participate, MRI contraindications, or absence of histopathological reports. MRI, performed on a 1.5 Tesla GE Signa HDxt scanner, used T1W, T2W, T2 FS, and post-contrast T1 FS sequences.

Lesions are diagnosed as benign when three of the four following criteria were met:

(a) Lesion size less than or equal to 4 cm in the largest diameter,

(b) entirely cystic,

(c) Lesion wall less than 3 mm thick,

(d) Lack of internal structure.

Prospective diagnosis of malignancy will be made when:

Lesion size was greater than 4 cm and either

(a) The lesion is cystic but wall thickness is greater than 3 mm and/or nodularity, vegetations, or a large solid component were present; or

(b) The lesion is completely or predominantly solid, with areas of necrosis or hemorrhage; or

(c) Any of the following findings were present:

-Involvement of adjacent pelvic organs,

-extension to the pelvic side walls, or

-presence of peritoneal, mesenteric, or omental disease, ascites, or adenopathy.

RESULTS

74 patients are included in the study and they had 88 lesions in total. Out of 74 patients 9 were having bilateral lesions and one of them had 5 lesions. Final diagnoses were made with the help of histopathology.76 lesions were proved to be benign lesions and 12 were under the category of malignant/probably malignant lesions.60 lesions were purely cystic lesions and the rest 28 lesions were either predominantly solid/ cystic lesions with solid components. In our study all the twelve histopathologically proven malignant lesions were detected on MRI as malignant/probably malignant lesions and no malignant lesion were misdiagnosed as benign neoplasm. However out of 14 lesions which have been diagnosed on MRI as malignant/ probably malignant lesions two lesions were found to be benign on histopathology. Remaining 74 lesions were found to benign on both MRI and histopathology. The sensitivity of MRI in detecting malignancy in ovarian tumours is calculated as 100% and specificity is calculated as 97.37%.

Table 1

Tumors	No of Lesions	Percentage of Total
Serous Cystadenomas	17	19.38%
Mucinous Cystaenomas	12	13.63%
Endometriomas	8	9.09%
Hemorrhagic Cysts	8	9.09%
Brenner Tumor	5	5.68%
Fibroma	4	4.54%
Fibrothecomas	2	2.27%
Dermoid Cyst	6	6.88%
Simple Follicular/Functional/Paraovarian Cysts	14	15.9%
Serous Cystadenocarcinomas	5	5.68%
Mucinous Cystadenocarcinomas	5	5.68%
Malignant Brenner	1	1.13%
Endometriod Cancer	1	1.13%

Benign Ovarian Lesions

1. Serous Cystadenoma (Cases 1-2): Two patients, aged 26 and 36 years, presented with abdominal pain. MRI demonstrated unilocular ovarian lesions that were T1-weighted (T1W) hypointense and T2-weighted (T2W) hyperintense with peripheral enhancement. In one case, multiple uterine fibroids were also observed. Histopathological analysis confirmed serous cystadenoma in both cases.

MRI Characteristics: Unilocular cystic lesions with peripheral enhancement and well-defined margins (Figure 1&2).

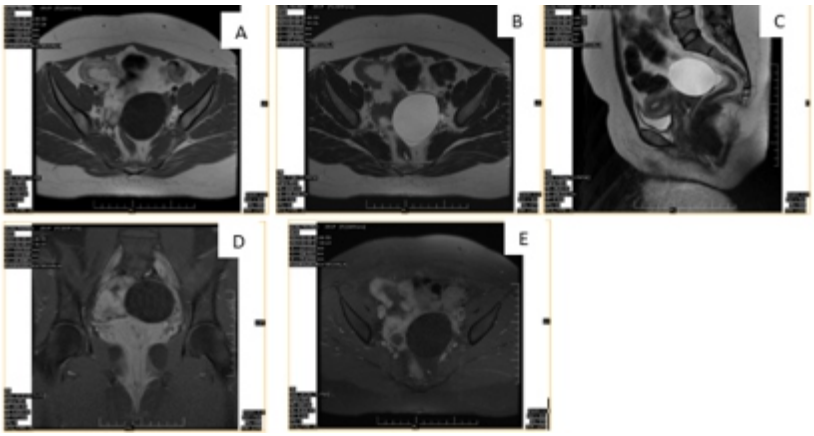

Figure 1: Histopathological Examination Confirmed the Lesion to be a Serous Cystadenoma

A: Axial T1W Image Showing Hypointense Unilocular Ovarian Lesion.

B: Axial T2W Image Depicting Hyperintense Lesion.

C: Sagittal T2W Image Highlighting Hyperintense Signal.

D: Coronal T1W Post-Contrast Image with Peripheral Enhancement.

E: Axial T1W Post Contrast Image Showing Peripheral Enhancement.

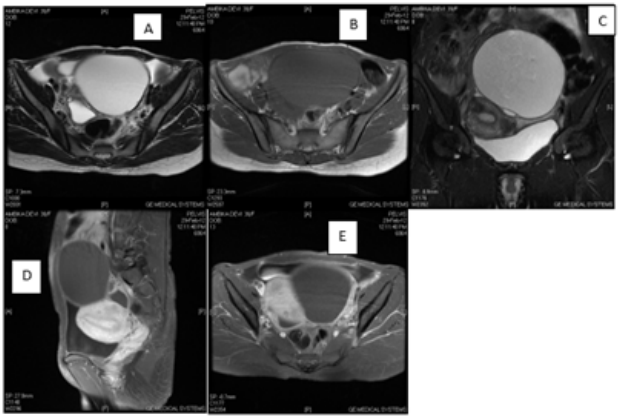

Figure 2: Histopathological Analysis Confirmed the Diagnosis of Serous Cystadenoma

A: Axial T2-Weighted Image Shows a Hyperintense Unilocular Lesion in the Left Ovary.
B: Axial T1-Weighted Image Displays a Hypointense Ovarian Lesion.
C: Coronal T2-Weighted Image Reveals Hyper Intense Lesion with no Septation.
D: Sagittal T1-Weighted Post Contrast Image Showing Peripheral Enhancement.
E: Axial T1 Weighted Post Contrast Image Showing Lesion with. Peripheral Enhancement.

2. Mucinous Cystadenoma (Cases 3-4):

Two patients, aged 50 and 23 years, presented with a palpable abdominal lump and abdominal distension, respectively. MRI revealed multiloculated cystic ovarian lesions with T1W hypointense and T2W hyperintense signals, accompanied by enhancing septal walls. Ascites was observed in one case. Histopathological evaluation confirmed mucinous cystadenoma.

MRI Characteristics: Multiloculated cystic morphology with hyperintense cystic components and enhancing septae (Figure 3,4).

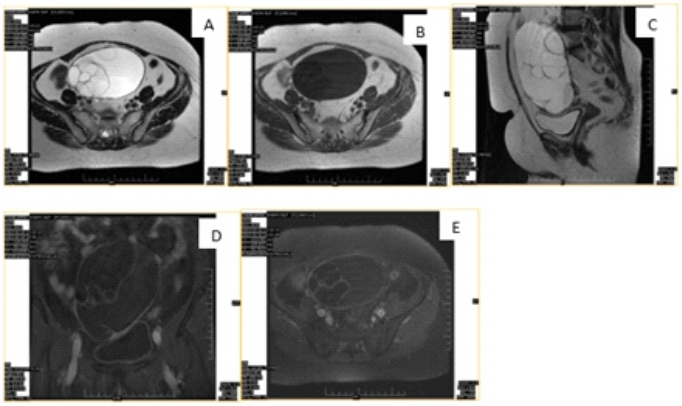

The Lesion and Its Spati
Structures.

Figure 3: Histopathology Confirmed the Diagnosis of Mucinous Cystadenoma

A: Axial T2-Weighted Image Showing a Multiloculated Cystic Lesion with Hyperintense Signal.
B: Axial T2-Weighted Image Demonstrating Hypointense Cystic Components.
C: Sagittal T2-Weighted Image Depicting the Extent of the Lesion and Its Spatial Relationship with Adjacent Structures.
D: Coronal T1- Weighted Post Contrast Image Showing Enhancing Septae Within Lesion.
E: Axial Post-Contrast T1-Weighted Image Highlighting Septal Enhancement Within the Lesion.

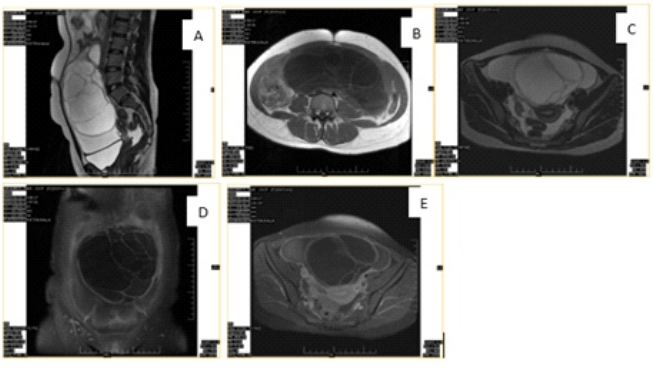

Figure 3: Histopathology Confirmed the Diagnosis of Mucinous Cystadenoma

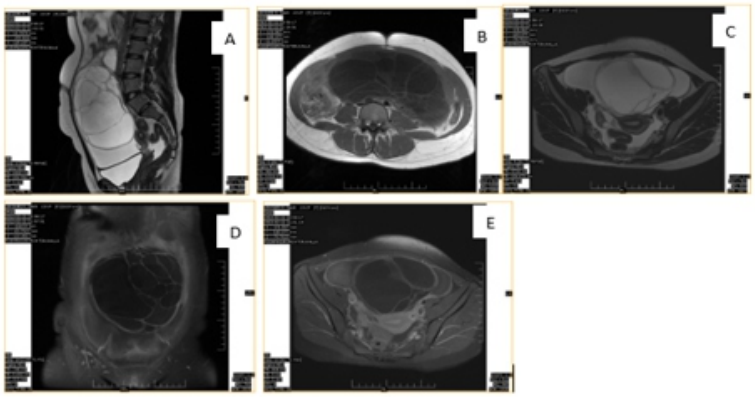

Figure 4: Histopathological Examination Confirmed the Diagnosis of Mucinous Cystadenoma

A: Sagittal T2W Image Showing a Multiloculated Hyperintense Lesion.
B: Axial T1W Image with Hypointense Cystic Components.
C: Axial T2W Image Highlighting Hyperintense Cystic areas.
D: Coronal T1- Weighted Post Contrast Image Showing Enhancing Septae within Lesion.
E: Axial Post-Contrast T1W Image with Enhancing Septal Walls.

3. Endometriotic and hemorrhagic Cysts (Cases 5-6):

Two patients, aged 44 and 29 years, presented with pelvic pain and irregular menstrual cycles, respectively. MRI identified multiloculated lesions with enhancing septae. One case displayed a "shade sign" on T2W imaging, and the other included bilateral ovarian cysts with hemorrhagic changes. Histopathology confirmed endometriotic cysts in both cases.

MRI Characteristics: Multiloculated lesions with hyperintense cystic components and enhancing septae (Figure 5& 6).

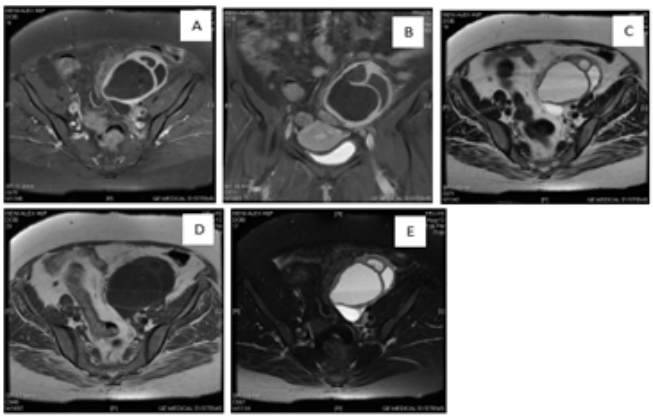

Figure 5: Histopathological Diagnosis: Endometriotic Cyst

A: Axial T1 Weighted Post Contrast Image Showing Multiolocular Lesion with Enhancing Septae.
B: Coroanl T1 Weighted Post Contrast Image Showing Multiolocular Lesion with Enhancing Septae.
C: Axial T2W Image with Hyperintense Cystic Components with Shade Sign.
D: Axial T1 W Image Showing Hypo Intense Cystic Lesion.
E: Axial T2W Fat Saturated Image Showing Shade Sign.

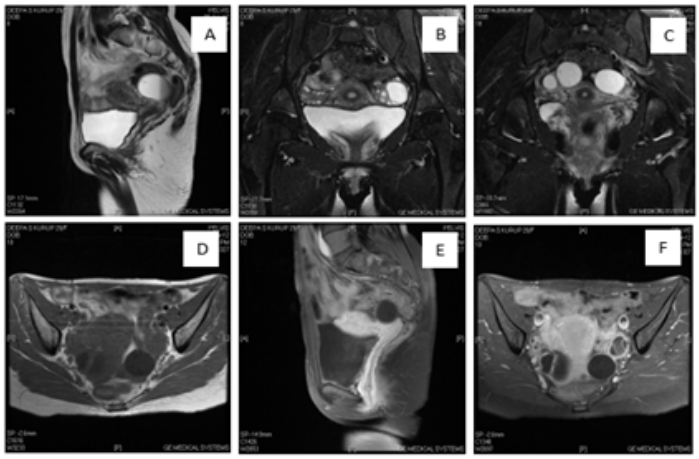

Figure 6: Diagnosis: Bilateral Simple Ovarian Cysts and Right Side Hemorrhagic Cyst

A: Sagittal T2W image showing a hyperintense cystic lesion with blood products in dependent part.
B: Coronal T2 Fat-Saturated image showing cystic lesion with blood product on right side.
C: Coronal T2W fat saturated image showing bilateral simple ovarian cysts.
D: Axial T1W post contrast image with hypointense cystic components.
E: Sagittal post-contrast T1W image showing no enhancement within the lesion.
F: Axial post-contrast T1W image with multiple cysts with no internal solid components.

4. Dermoid Cyst (Case 7): A 17-year-old female presented with lower abdominal pain. MRI demonstrated a predominantly solid lesion in the left ovary, characterized by mixed T1W and T2W signals with central fat suppression. Histopathology confirmed a dermoid cyst with a dermoid plug.

MRI Characteristics: Mixed solid-cystic lesion with distinct cystic and solid components (Figure 7).

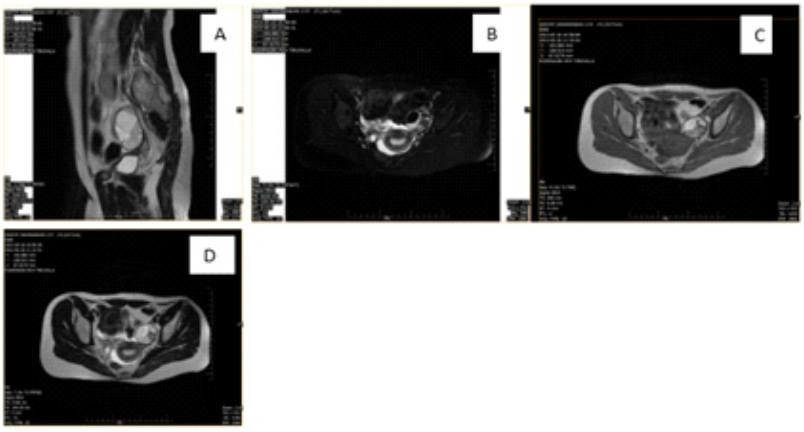

Figure 7: Histopathological Diagnosis: Dermoid Cyst.

A: Sagittal T2W image showing a hyperintense lesion with solid component.
B: Axial T2 Fat-Saturated image highlighting fat suppression of solid component.
C: Axial T1W image illustrating hyperintense solid component with in the cyst.
D: Axial T2W image demonstrating hyperintense lesion with solid component.

5. Fibroma and Fibrothecoma (Cases 8-9): Two patients, aged 36 and 39 years, presented with abdominal distension and menorrhagia, respectively. MRI revealed solid-cystic ovarian lesions with intermediate T1W and high T2W signals, along with multiloculated morphology and peripheral enhancement. Histopathology confirmed fibrothecoma and fibroma, respectively.

MRI Characteristics: Solid-cystic lesions with enhancing solid components and hyperintense cystic regions (Figure 8&9).

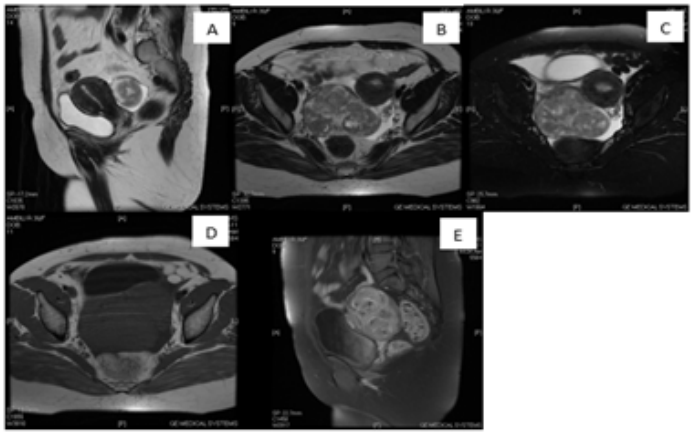

Figure 8: Histopathological Diagnosis: Fibrothecoma

A: Sagittal T2W image showing a solid-cystic lesion with hyperintense cystic components.
B: Axial T2W image illustrating heterogenous predominantly high signal.
C: Axial T2 Fat-Saturated image highlighting hyperintense cystic components.
D: Axial T1W image demonstrating isointense signal of the lesion.
E: Sagittal T1W post contrast mage showing the hetrogenously enhancing lesion

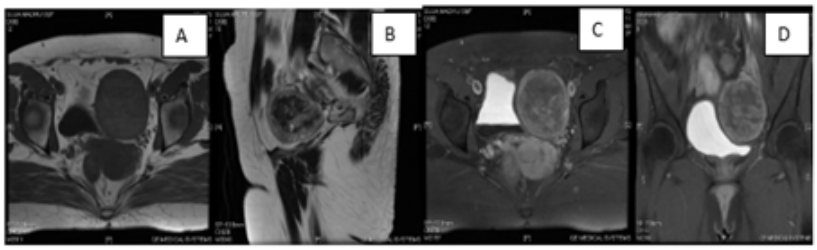

Figure 9: Histopathological Diagnosis: Fibroma

A: Axial T1W image showing a solid isointense lesion in the pelvis.
B: Sagittal T2W image illustrating peripheral hyperintense and central hypointense areas within the lesion.
C: Axial T1w post-contrast T1W image highlighting intense peripheral enhancement.
D: Coronal T1w post-contrast T1W image highlighting intense peripheral enhancement.

6. Benign Brenner Tumor (Case 10):

A 47-year-old female presented with abdominal discomfort and pain. MRI revealed a right pelvic lesion with T2W hypointense signals, causing mass effect on adjacent bowel loops and the urinary bladder. The lesion exhibited mixed solid-cystic characteristics. Histopathology confirmed a benign Brenner tumor.

MRI Characteristics: T2W hypointense solid-cystic lesion.

- Mass effect on adjacent structures without evidence of invasion. (Figure 10)

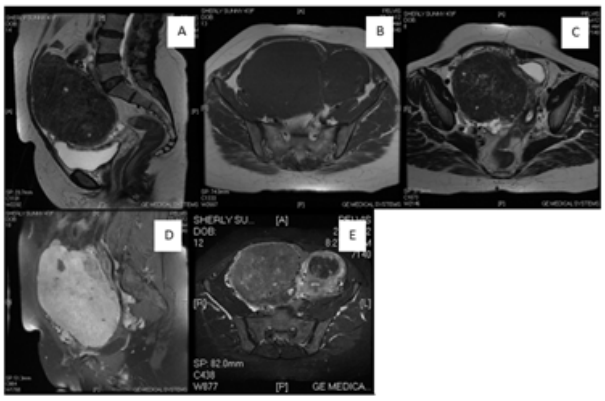

Figure 10: Histopathological Diagnosis: Benign Brenner Tumor

A: Sagittal T2W image showing a large solid lesion with hypo intense signal
B: Axial T1W image displaying a isointense lesion.
C: Axial T2W image illustrating hypointense lesion.
D: Sagittal post-contrast T1W image demonstrating intense enhancement in the solid component.
E: Axial post-contrast T1W image demonstrating intense enhancement in the solid component.

2. Malignant Ovarian Lesions

1. Serous and mucinous Cystadenocarcinoma (Cases 11-12):

Two patients, aged 64 and 59 years, presented with abdominal discomfort and distension. MRI demonstrated large mixed solid-cystic lesions with intermediate T1W and high T2W signals, along with peritoneal deposits, lymphadenopathy, and ascites. Elevated CA-125 levels were noted in one case. Histopathology confirmed serous cystadenocarcinoma in both cases.

MRI Characteristics:

- Mixed solid-cystic lesions with enhancing solid and septal components.
- Peritoneal involvement and ascites. (Figure 11& 12)

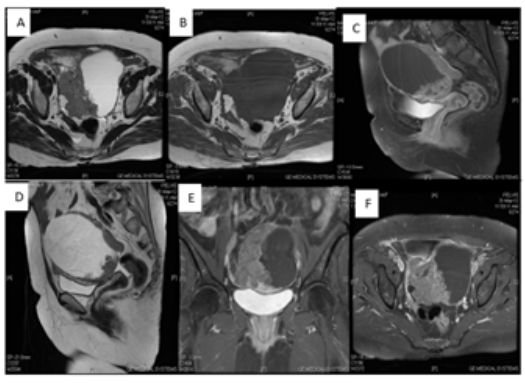

Figure 11: Multimodal MRI Imaging of Serous Cystadenocarcinoma Ovary

A: Axial T2-weighted image showing a solid cystic lesion.
B: Axial T1-weighted image demonstrating intermediate signal
C: Sagittal T1-weighted post contrast image depicting the serosal deposits along recto sigmoid junction.
D: Sagittal T2 weighted image showing a hyperintense cystic lesion with solid component within.
E: Coronal post-contrast T1-weighted image showing enhancement of solid component.
F: Axial post-contrast image revealing enhancement of solid component.

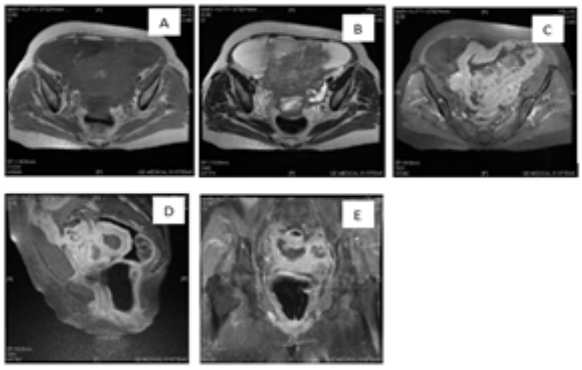

Figure 12: Histopathological Diagnosis: Mucinous Cystadenocarcinoma

A: Axial T1W image showing a mixed signal lesion with ascites.
B: Axial T2W image demonstrating cites and complex left adnexal hyperintense lesion.
C: Axial post-contrast T1W image highlighting enhancing solid component, ascites, peritonealdeposits.
D: Sagittal post-contrast T1W image highlighting enhancing solid component, ascites, peritonealdeposits.
E: Coronal post-contrast T1W image highlighting enhancing solid component, ascites, peritonealdeposits.

2. Malignant Brenner Tumor (Case 13):

A 68-year-old female presented with abdominal pain. MRI revealed a heterogeneously enhancing mixed lesion that was isointense on T1W and hyperintense on T2W imaging. Histopathology confirmed a malignant Brenner tumor.

MRI Characteristics: Multiloculated morphology with significant septal and solid enhancement (Figure 13)

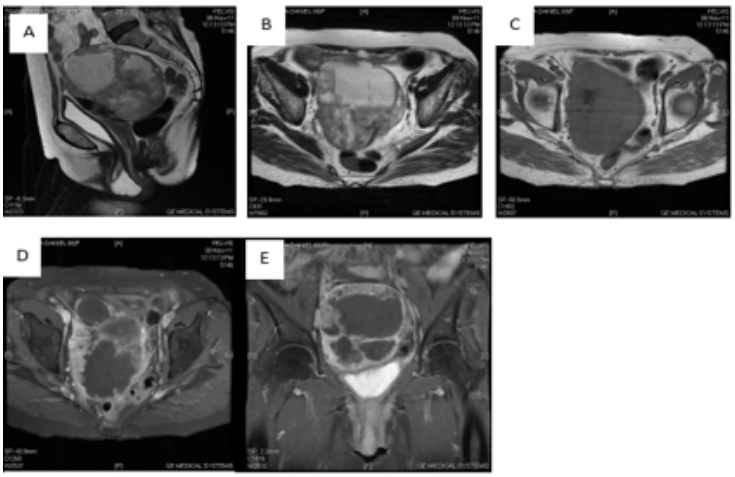

Figure 13: Histopathological Diagnosis: Malignant Brenner Tumor

A: Sagittal T2W image showing a large multiloculated lesion with hyperintense cystic areas.
B: Axial T2W image demonstrating heterogeneous lesion with hyper intense cystic components.
C: Axial T1W image highlighting isointense cystic component.
D: Axial post-contrast T1W image showing significant enhancement of the septal and solid components.
E: Coronal post-contrast T1W image showing significant enhancement of the septal and solid components.

3. Endometrioid Adenocarcinoma (Case 14):

A 65-year-old female presented with menorrhagia and abdominal distension. MRI revealed a solid-cystic ovarian lesion with enhancing solid components and ascites. Histopathological analysis confirmed endometrioid adenocarcinoma.

MRI Characteristics: Solid-cystic lesion with hyperintense cystic areas, enhancing septae, and ascites (Figure 14)

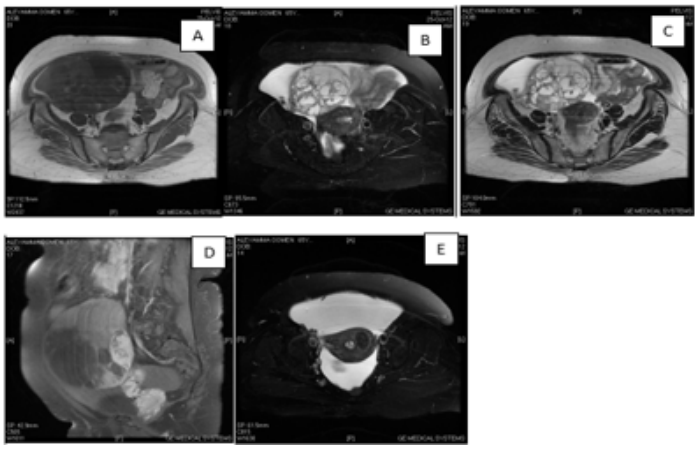

Figure 14: MRI Imaging of an Ovarian Lesion

A: Axial T1-weighted image showing a hypointense lesion.
B: Axial T2 Fat-Saturated image demonstrating hyperintense signal within the lesion.
C: Axial T2-weighted image depicting lesion characteristics with clear septations.
D: Sagittal T1 weighted post contrast image highlighting areas of septal and solid component enhancement.
E: Axial T2 weighted fat saturated image showing ascites, fibroid and cystic endometrial hyperplasia.

3. False Positive Case

Two patients, aged 26 and 43 years, presented with abdominal discomfort and lower abdominal pain, respectively. MRI revealed multiloculated cystic lesions with enhancing septae and papillary projections, initially suggestive of malignancy. However, histopathology confirmed benign serous cystadenoma in both cases. **MRI Characteristics:** Large multiloculated cystic lesions with enhancing septae and papillary projections.
Absence of invasive features (Figure 15&16)

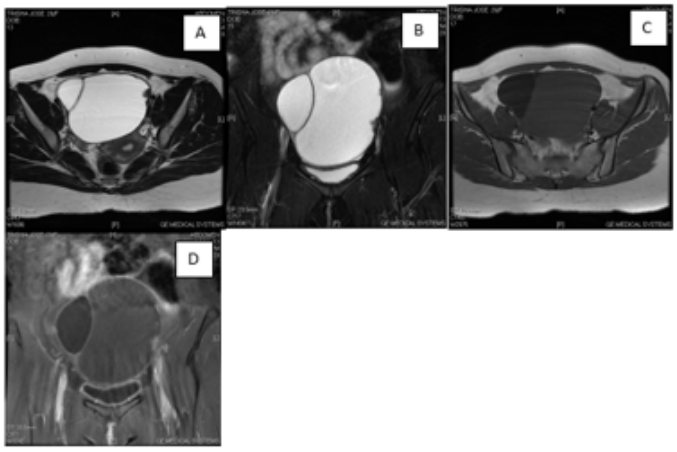

Figure 15: MRI Imaging of an Ovarian Lesion

A: Axial T2-weighted image showing a hyperintense mulitlocular cystic lesion with papillary projection.
B: Coronal T2-weighted image demonstrating hyperintense mulitlocular cystic lesion with papillary projection.
C: Axial T1weighted image showing the isoinense cystic lesion.
D: Coronal post-contrast T1-weighted image highlighting peripheral enhancement of the lesion.

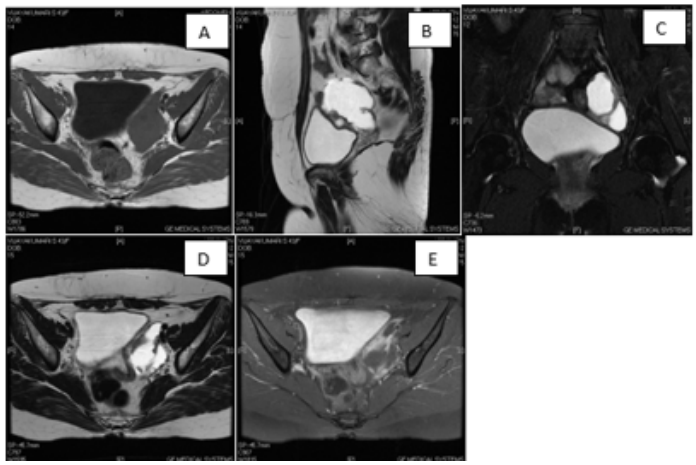

Figure 16: Multimodal MRI Imaging of a Pelvic Lesion

A: Axial T1-weighted image displaying a hypointense lesion.
B: Sagittal T2-weighted image illustrating the lesion with thick wall and septation.
C: Coronal T2-weighted image demonstrating a hyperintense lesion with thick wall and septation.
D: Axial T2-weighted image showing cystic characteristics of the lesion.
E: Axial post-contrast T1-weighted image highlighting areas of enhancement within the lesion.

DISCUSSION

Magnetic resonance imaging (MRI) is a critical tool in the differentiation of benign and malignant ovarian tumors, offering detailed morphological and functional insights that guide clinical decision-making [14]. This study demonstrates the efficacy of MRI in characterizing ovarian lesions by leveraging its superior soft-tissue contrast, multiplanar imaging capabilities, and ability to assess tissue vascularity through gadolinium enhancement. Consistent with findings by Stevens et al. (1991), this study found that benign lesions, such as serous cystadenomas, typically exhibited unilocular morphology, thin walls, and peripheral enhancement, while malignant lesions, including serous cystadenocarcinomas, displayed irregular walls, thick septae, solid enhancing components, and ancillary features such as ascites and peritoneal involvement [11].

The study's findings align with the multivariate approach highlighted by Hricak et al. (2000), emphasizing lesion size, morphology, signal intensity, and enhancement patterns as reliable parameters for classification [15]. Benign lesions like mucinous cystadenomas were characterized by multiloculated cystic morphology with hyperintense T2-weighted (T2W) signals and thin, enhancing septae. Similarly, endometriotic cysts displayed the characteristic "shade sign" on T2W imaging, as described by Togashi et al. (1991) [12]. In contrast, malignant lesions exhibited heterogeneous signal intensities, irregular septae, and solid components, often accompanied by elevated CA-125 levels, as seen in serous cystadenocarcinoma cases.

Specific imaging features of ovarian tumor subtypes in this study are consistent with established literature. Germ cell tumors, such as dermoid cysts, demonstrated mixed T1-weighted (T1W) and T2W signals with fat suppression, aligning with descriptions by Talerman (2002). Surface epithelial tumors like serous and mucinous cystadenomas exhibited smooth, well-defined margins, while their malignant counterparts showed invasive features, including thick septae, solid components, and peritoneal involvement, as noted by Seidman et al. (2002) [16]. Furthermore, fibromas and fibrothecomas displayed hypointense T2W signals with peripheral enhancement, corroborating the findings of Schwartz et al. (1997) [17]. Endometriotic lesions, although predominantly benign in this study, warrant attention due to their potential association with epithelial ovarian cancer, as reported by Jimbo et al. (1997) [18].

The role of diffusion-weighted imaging (DWI) as an adjunct to traditional sequences is increasingly recognized in ovarian tumor evaluation. Studies by Tanaka et al. (2000) and Outwater et al. (1998) have shown that DWI adds value by quantifying tissue cellularity and distinguishing between benign and malignant lesions based on apparent diffusion coefficient (ADC) value [19,20]. In this context, malignant lesions tend to exhibit restricted diffusion with low ADC values, a feature that could complement morphological findings in differentiating complex adnexal masses. Incorporating DWI into routine MRI protocols may further reduce diagnostic ambiguity and improve the specificity of MRI.

Gadolinium-enhanced MRI proved invaluable in highlighting vascularity and enhancement patterns, distinguishing benign lesions with peripheral enhancement from malignant lesions with heterogeneous enhancement in solid and septal components. However, as observed in this study and noted by Outwater et al. (1998), false-positive cases occurred when benign lesions mimicked malignancy due to overlapping imaging features like multiloculation, papillary projections, and septal enhancement [20]. These instances underscore the necessity of histopathological confirmation to establish a definitive diagnosis.

This study highlights the clinical utility of MRI in preoperative evaluation and risk stratification of ovarian tumors, reducing unnecessary surgical interventions while facilitating appropriate treatment planning. While its non-invasive nature and high diagnostic accuracy make MRI an essential tool, limitations such as a small sample size and potential contraindications to gadolinium use warrant consideration. Advanced imaging techniques, including diffusion-weighted imaging (DWI) and dynamic contrast-enhanced (DCE) MRI, could further enhance diagnostic precision in future studies. Overall, the integration of MRI findings with histopathological evaluation remains crucial for ensuring accurate diagnosis and optimal patient management.

CONCLUSION

Magnetic resonance imaging (MRI) is a crucial tool for differentiating benign and malignant ovarian tumors, offering high sensitivity and specificity. This study demonstrated the utility of MRI in characterizing lesions based on morphology, enhancement patterns, and signal intensity. Gadolinium-enhanced imaging effectively detected malignancy, though occasional false positives necessitate histopathological confirmation. MRI's integration into preoperative planning reduces unnecessary surgeries and improves outcomes. Future advancements, including artificial intelligence, promise to refine ovarian tumor evaluation, solidifying MRI's role as an essential modality in diagnosis and management.

REFERENCES

1. Huang J, Chan WC, Ngai CH, Lok V, Zhang L, Lucero-Prisno DE, et al. Worldwide Burden, Risk Factors, and Temporal Trends of Ovarian Cancer: A Global Study. Cancers (Basel) Internet. 2022 Apr 29 cited 2025 Jan 10;14(9):2230. Available from: https://www.ncbi.nlm.nih.gov/pmc/articles/PMC9102475/
2. Basu P, De P, Mandal S, Ray K, Biswas J. Study of 'patterns of care' of ovarian cancer patients in a specialized cancer institute in Kolkata, eastern India. Indian Journal of Cancer [Internet]. 2009 Mar [cited 2025 Jan 10];46(1):28. Available from: https://journals.lww.com/indianjcancer/fulltext/2009/46010/ Study of patterns of careo fo varian cancer.5.aspx
3. Koutras A, Perros P, Prokopakis I, Ntounis T, Fasoulakis Z, Pittokopitou S, et al. Advantages and Limitations of Ultrasound as a Screening Test for Ovarian Cancer. Diagnostics [Internet]. 2023 Jan [cited 2025 Jan 10];13(12):2078. Available from: https://www.mdpi.com/2075-4418/13/12/2078
4. Avesani G, Panico C, Nougaret S, Woitek R, Gui B, Sala E. ESR Essentials: characterisation and staging of adnexal masses with MRI and CT-practice recommendations by ESUR. Eur Radiol [Internet]. 2024 Dec 1 [cited 2025 Jan 10];34(12):7673-89. Available from: https://doi.org/10.1007/s00330-024-10817-1
5. Nikolic O, Basta Nikolic M, Spasic A, Otero-Garcia MM, Stojanovic S. Systematic radiological approach to utero-ovarian pathologies. Br J Radiol [Internet]. 2019 Jul [cited 2025 Jan 10];92(1099):20180439. Available from: https://www.ncbi.nlm.nih.gov/pmc/articles/PMC6636271/
6. Valentini AL, Gui B, Miccò M, Mingote MC, De Gaetano AM, Ninivaggi V, et al. Benign and Suspicious Ovarian Masses-MR Imaging Criteria for Characterization: Pictorial Review. J Oncol [Internet]. 2012 [cited 2025 Jan 10];2012:481806. Available from: https://www.ncbi.nlm.nih.gov/pmc/articles/PMC3321462/
7. Sohaib SAA, Reznek RH. MR imaging in ovarian cancer. Cancer Imaging [Internet]. 2007 Oct 1 [cited 2025 Jan 10];7(Special issue A):S119–29. Available from: https://www.ncbi.nlm.nih.gov/pmc/articles/PMC2727977/
8. Koch AH, Jeelof LS, Muntinga CLP, Gootzen TA, van de Kruis NMA, Nederend J, et al. Analysis of computer-aided diagnostics in the preoperative diagnosis of ovarian cancer: a systematic review. Insights into Imaging [Internet]. 2023 Feb 15 [cited 2025 Jan 10];14(1):34. Available from: https://doi.org/10.1186/s13244-022-01345-x
9. Kido A, Togashi K, Konishi I, Kataoka ML, Koyama T, Ueda H, et al. Dermoid cysts of the ovary with malignant transformation: MR appearance. AJR Am J Roentgenol. 1999 Feb;172(2):445-9.
10. Jeong YY, Outwater EK, Kang HK. Imaging Evaluation of Ovarian Masses. RadioGraphics [Internet]. 2000 Sep [cited 2025 Jan 10];20(5):1445-70. Available from: https://pubs.rsna.org/doi/10.1148/radiographics.20.5.g00se101445
11. Stevens SK, Hricak H, Stern JL. Ovarian lesions: detection and characterization with gadolinium-enhanced MR imaging at 1.5 T. Radiology. 1991 Nov;181(2):481-8.
12. Togashi K, Nishimura K, Kimura I, Tsuda Y, Yamashita K, Shibata T, et al. Endometrial cysts: diagnosis with MR imaging. Radiology. 1991 Jul;180(1):73-8.
13. Valentini AL, Gui B, Miccò M, Mingote MC, De Gaetano AM, Ninivaggi V, et al. Benign and Suspicious Ovarian Masses-MR Imaging Criteria for Characterization: Pictorial Review. J Oncol [Internet]. 2012 [cited 2025 Jan 10];2012:481806. Available from: https://www.ncbi.nlm.nih.gov/pmc/articles/PMC3321462/
14. Behnamfar F, Tashakor Z, Adibi A. Magnetic Resonance Imaging Findings in Patients with Benign and Malignant Ovarian Masses Versus Pathologic Outcomes. Adv Biomed Res [Internet]. 2020 Oct 30 [cited 2025 Jan 10];9:64. Available from: https://www.ncbi.nlm.nih.gov/pmc/articles/PMC7792878/
15. Hricak H, Chen M, Coakley FV, Kinkel K, Yu KK, Sica G, et al. Complex adnexal masses: detection and characterization with MR imaging--multivariate analysis. Radiology. 2000 Jan;214(1):39–46.
16. Seidman JD, Cho KR, Ronnett BM, Kurman RJ. Surface Epithelial Tumors of the Ovary. In: Kurman RJ, Ellenson LH, Ronnett BM, editors. Blaustein's Pathology of the Female Genital Tract [Internet]. Boston, MA: Springer US; 2011 [cited 2025 Jan 10]. p. 679-784. Available from: https://doi.org/10.1007/978-1-4419-0489-8_14
17. Schwartz RK, Levine D, Hatabu H, Edelman RR. Ovarian fibroma: findings by contrast-enhanced MRI. Abdom Imaging. 1997;22(5):535-7.
18. Jimbo H, Yoshikawa H, Onda T, Yasugi T, Sakamoto A, Taketani Y. Prevalence of ovarian endometriosis in epithelial ovarian cancer. Int J Gynaecol Obstet. 1997 Dec;59(3):245-50.
19. Tanaka YO, Nishida M, Yamaguchi M, Kohno K, Saida Y, Itai Y. MRI of gynaecological solid masses. Clin Radiol. 2000 Dec;55(12):899-911.
20. Outwater EK, Siegelman ES, Chiowanich P, Kilger AM, Dunton CJ, Talerman A. Dilated fallopian tubes: MR imaging characteristics. Radiology. 1998 Aug;208(2):463-9.

How to cite: Kabil Kumar. Role of MRI in Differentiating Benign and Malignant Ovarian Tumors. *International Medicine, 2025;11 (1):1-11.*